Studies on preparation and characterisation of 45S5 bioactive glass doped with (TiO_2+ ZrO_2) as bioactive ceramic material

7.1. Introduction

Bioactive glasses have been widely investigated for bone repair because of their outstanding bioactive properties. However, these bioactive materials undergo incomplete conversion into a bone-like material which severely limits their biomedical application (Hench, 1991). When bioactive glasses are soaked in simulated body fluid, they bind to living bone through an apatite layer formed on their surfaces. The mechanism of the reaction for bonding the implant to the bone was given by Clark and Hench (Clark and L.L. Hench, 1976). One of the main characteristics of the bioactive glasses is their highly reactive surface. Hench decided to make a glass in the SiO_2-Na_2O-CaO-P_2O_5 system, high in calcium content and with a composition close to a ternary eutectic in the Na_2O–CaO–SiO_2 diagram (Hench, 2006). The main discovery was that a glass of the mol% composition 46.1 SiO_2, 24.4 Na_2O, 26.9 CaO and 2.6 P_2O_5, later termed 45S5 and Bioglass, formed a bond with the bone so strong that it could not be removed without breaking the bone (Hench *et al*., 1971). This launched the field of bioactive ceramics, with many new materials and products being formed from variations on bioactive glasses (Hench, 2006), glass–ceramics (Kokubo, 1991) and ceramics such as synthetic hydroxyapatite (HA) and other calcium phosphates (LeGeros, 2002). Herein, a bioactive material is defined as a material that stimulates a beneficial response from the body, particularly bonding to host tissue (usually bone). The term ‘‘bioceramic’’ is a general term used to cover glasses, glass–ceramics and ceramics that are used as implant

materials. Bioglass 45S5 is widely used in biomedical devices, such as middle ear and dental implants. However, its relatively low strength and brittleness limit its application to non-load-bearing situations (Cao *et al*., 1996). There are now several types of bioactive glasses: the conventional silicates, such as Bioglass 45S5; phosphate-based glasses; and borate-based glasses. Recently, interest has increased in borate glasses (Rahaman *et al*., 2011), largely due to very encouraging clinical results of healing the chronic wounds, such as diabetic and ulcers, which would not heal under conventional treatment (Jung *et al*., 2011). The soft tissue response may be due to their fast dissolution, which is more rapid than that for silica-based glasses. The benefits of phosphate glasses are also likely to be related to their very rapid solubility rather than bioactivity (Abou Neel *et al*., 2009).

In order to improve the mechanical reliability of glass-based biomedical devices, various approaches have been proposed, such as the production of sintered bodies or the deposition of coatings. However, the BG-45S5, like other bioactive glasses, tends to crystallize at high temperature, due to its relatively low content of silica (Arstila *et al*., 2008). This is a relevant drawback since the crystallization is thought to reduce the bioactivity of the glass (Shirtliff *et al*., 2003 and Li *et al*., 1992) and, on the other hand, thermal treatments are widely required to obtain not only special products, such as sintered glass scaffolds or glass fibers but also ordinary coatings (Arstila *et al*., 2008). The addition of elements like magnesium, aluminum, zirconia, or titanium may be used to control some physical and chemical properties of bioglasses (Agathopoulos *et al*., 2006 and Marti, 2000). When the bioglass is doped with TiO_2, the apatite can be formed biomimetically on the surface of bioglass immersed in simulated body fluid. Titania has a tendency to adsorb water at the surface, resulting in the formation of titanium hydroxide

groups. The basic Ti-OH groups were reported to induce apatite nucleation and crystallization in simulated body fluid (Bharati *et al*., 2009). The production of composite materials has proved to be the suitable solutions for improving the mechanical properties of weaker materials. Ceramic biocomposites were reinforced by introducing another tough phase of Al_2O_3 and ZrO_2 (Marti, 2000). The yttria-stabilized zirconia was introduced into orthopedic surgery in the late eighties as a new generation ceramic material (Habibe *et al*., 2009). Zirconia is particularly attractive as a reinforcing phase since it is bio-inert and HA/ZrO_2 composites give significantly improved mechanical properties (Singh *et al*., 2006).

Therefore, in the present investigation, the 45S5 bioactive glass has been taken as a reference. The concentration of SiO_2 was varied by mol% addition of (TiO_2+ZrO_2) in the ratio of (3:2) from 1-4 mol%, respectively in the 45S5 bioactive glass. The purpose of this work is to provide information on bioactivity assessment and to increase the other physical and mechanical properties of 45S5 bioactive glass by introducing 1-4 mol% (TiO_2+ZrO_2) into it.

7.2. Materials and methods

7.2.1 Sample preparation

The mol% compositions of the bioglass samples are shown in Table 7.1. Fine-grained quartz was used for silica (SiO_2). Analytical reagent grade calcium carbonate ($CaCO_3$), sodium carbonate (Na_2CO_3) and ammonium dihydrogen orthophosphate ($NH_4H_2PO_4$) (Merck specialities private limited, Mumbai, India, Assay 99.8%) were used as a source of CaO, Na_2O and P_2O_5, respectively. The required amounts of analytical reagent grade (Merck specialities private limited, Mumbai, India, Assay 99.8%) TiO_2 and ZrO_2 were

added in the batch for the partial substitution of silica. The proper raw materials for different samples were weighted. Then the mixing of different batches was done for 30 minutes and melted in alumina crucibles. The thermal cycle was set for all glass samples: from room temperature to 1000 ^{0}C at 10^{0}C/min; at 1000 ^{0}C for 1 hour; from 1000^{0}C to 1400^{0}C at 10^{0}C/min; at 1400^{0}C for 2 hours. The melting of samples was done in the electronic globar furnace, air as the furnace atmosphere. The melted samples were poured on a preheated aluminum sheet and directly transferred to a regulated muffle furnace at 450 ^{0}C for annealing and after 1 hour of annealing of the samples, muffle furnace was cooled to the room temperature at the rate of 15^{0}C/hr. The other parts of the samples were crushed in a pestle mortar and then ground in an agate mortar to make fine powders for measurements of its bioactivity in SBF and other properties using various experimental techniques such as XRD, FTIR spectrometry, SEM analysis and pH measurements. The other half of solid glass samples were used for density and compressive strength measurements.

Table 7.1: Mol% composition of bioactive glass samples.

Sl No.	SAMPLE	SiO_2	Na_2O	CaO	P_2O_5	(TiO_2+ZrO_2) (3:2)
1.	45S5	46.1	24.4	26.9	2.6	0
2.	TZ1	45.1	24.4	26.9	2.6	1
3.	TZ2	44.1	24.4	26.9	2.6	2
4.	TZ3	43.1	24.4	26.9	2.6	3
5.	TZ4	42.1	24.4	26.9	2.6	4

7.2.2 In-vitro analysis of bioactive glass samples

The *in vitro* bioactivity assessments of the glasses were carried out by their immersion in simulated body fluid (SBF) solutions for 1 to 28 days at 37.4°C. The simulated body fluid (SBF) solutions were prepared according to the formula described by Kokubo *et al* (Kokubo *et al*., 1990). Table 7.2 shows the ion concentrations of the SBF solution.The glass samples in the form of palate having the size of 1 cm diameter were immersed in SBF at 37.4 ^{0}C for different time periods varying from 1 to 28 days. The pH of the SBF solutions was measured using digital pH meter for different time periods.

Table 7.2: The ions concentration of the SBF solution (mM/l).

Sl no.	Ion	Concentration (mM/l)
1.	Na^{+}	142.0
2.	K^{+}	5.0
3.	Mg^{2+}	1.5
4.	Ca^{2+}	2.5
5.	Cl^{-}	147.8
6.	HCO_3^{-}	4.2
7.	HPO_4^{2-}	1.0
8.	SO_4^{2-}	0.5

7.2.3 Structural analysis of bioglasses by FTIR transmittance spectroscopy.

The in-vitro bioactivity of chemically treated samples in SBF solution was assessed by evaluating the formation of carbonated hydroxy calcium phosphate layer on the surface of the samples before and after immersion in SBF solution using FTIR transmittance spectroscopy. The infrared transmittance spectra of the bioglasses were recorded at the room temperature in the spectral range 4000-400 cm^{-1} using a Fourier Transform Infra-Red spectrometer (Shimadzu-8400S**,** Japan).

7.3. Results and discussion

7.3.1 Density and compressive strength of bioactive glass samples

The results in Table 7.3 show the density and Fig. 7.1 shows the compressive strength of bioactive glass samples in the form of error bars.

Table 7.3: Density of bioactive glass samples (gm/cc).

Serial No.	Sample's Name	Density (gm/cc)
1	45S5	2.54
2	TZ1	2.70
3	TZ2	2.76
4	TZ3	2.80
5	TZ4	2.89

It is observed that the densities of the samples were found to increase with increasing (TiO_2+ZrO_2) content in the glass from 2.54 to 2.89 gm/cc with the increasing amount of (TiO_2+ZrO_2) contents into the bioactive glass samples.

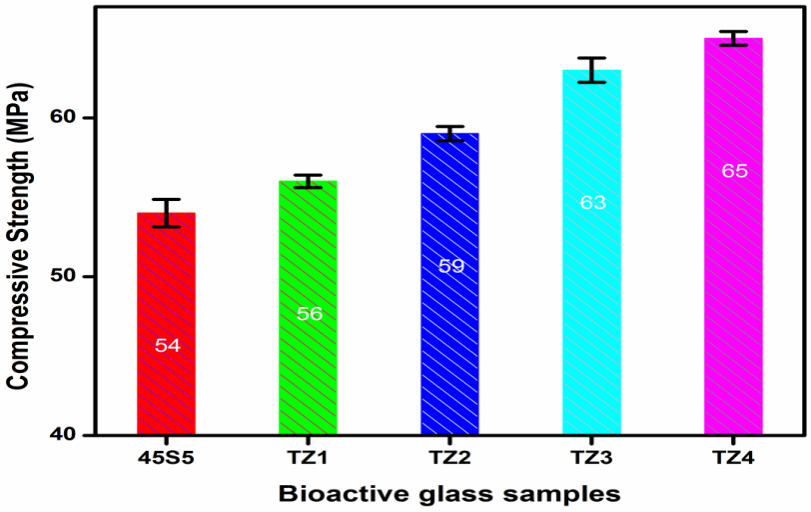

Fig. 7.1: Variation of compressive strength with composition of the bioactive glass samples (45S5 to TZ4).

From the Fig. 7.1, it is also clear that with the increasing amount of (TiO_2+ZrO_2) the compressive strength of samples has increased from 54 to 65 MPa.

It may be due to partial replacement of SiO_2 with (TiO_2+ZrO_2) which is attributed due to the replacement of a smaller ion (Si^{4+}) with a bigger Ti^{2+} and Zr^{2+} ions in the glass. In other words, the lighter molar mass of SiO_2 (60.08 g/mol) has been replaced by the heavier TiO_2 (79.86 gm/mol) and ZrO_2 (123.22 gm/mol) in the bioactive glass samples.

7.3.2 X-Ray Diffraction analysis of bioactive glass samples.

X-ray diffraction patterns were observed using a Rigaku portable XRD machine (Rigaku, Tokyo, Japan). Phase identification analysis was carried out by comparing the XRD patterns of the bioactive glass samples to the standard database stated by JCPDF which is indicated in Fig. 7.2.

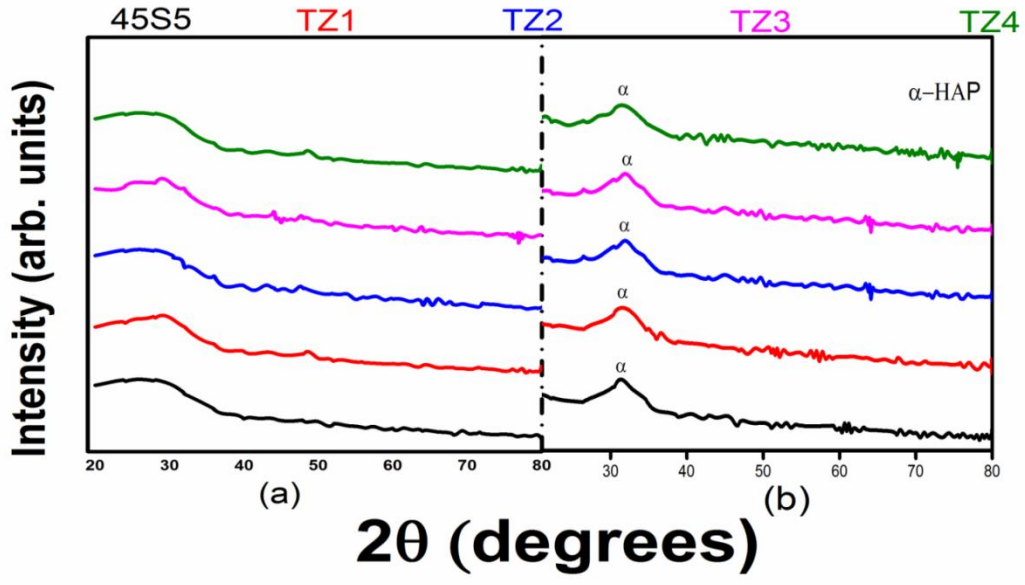

Fig. 7.2: (a) XRD patterns of bioactive glass samples (45S5 to TZ4) before immersing the samples in SBF. (b) XRD patterns of bioactive glass samples (45S5 to TZ4) after immersing the samples in SBF for 14 days.

Fig. 7.2 (a) shows the XRD plots of the bioactive glass samples before soaking them into the simulated body fluid (SBF). Before being soaked in SBF solutions, there was no XRD absorption peak for the bioactive glass samples, except for one bump like peak ranging from 20° to 30°, which is due to Si-O-Si network (Tripathi *et al*., 2016). So it is clear that bioactive glass samples were amorphous in nature before being soaked in simulated body fluid (SBF) solution. While Fig. 7.2 (b) shows the XRD plots of the bioactive glass samples soaked in the simulated body fluid (SBF) solution for 14 days. After being soaked in the SBF solution for 14 days, one diffraction peak was observed at a 2θ angle of 31.9°, corresponding to the HA phase. These peaks were identified by standard JCPDS cards numbered 89-6495.

7.3.3 In-vitro analysis of bioactive glass samples

Fig. 7.3 shows the variation of pH of bioactive glass samples after immersing in simulated body fluid (SBF) solution for 1 to 28 days. Greenspan *et al*. (Greenspan and Hench, 1976) also confirmed that changes in pH of glass samples took place after immersion in simulated body fluid (SBF) solution. It shows that for all bioactive glass samples, the pH increases within 1 to 7 days as compared to the initial pH of the SBF solution at 7.4. The increase in pH values is due to the fast release of Na^{+} and Ca^{++} ions through exchange with H^{+} or H_3O^{+} ions into the simulated body fluid (SBF) solution. The H^{+} ions are being replaced by cations which cause an increase in hydroxyl concentration of the solution. This leads to attack in the silica glass network, which results in the formation of silanols leading to decrease in pH which is indicated in the Fig. 7.3 as

bioactive glass samples immersed in simulated body fluid (SBF) solution for 7 to 28 days.

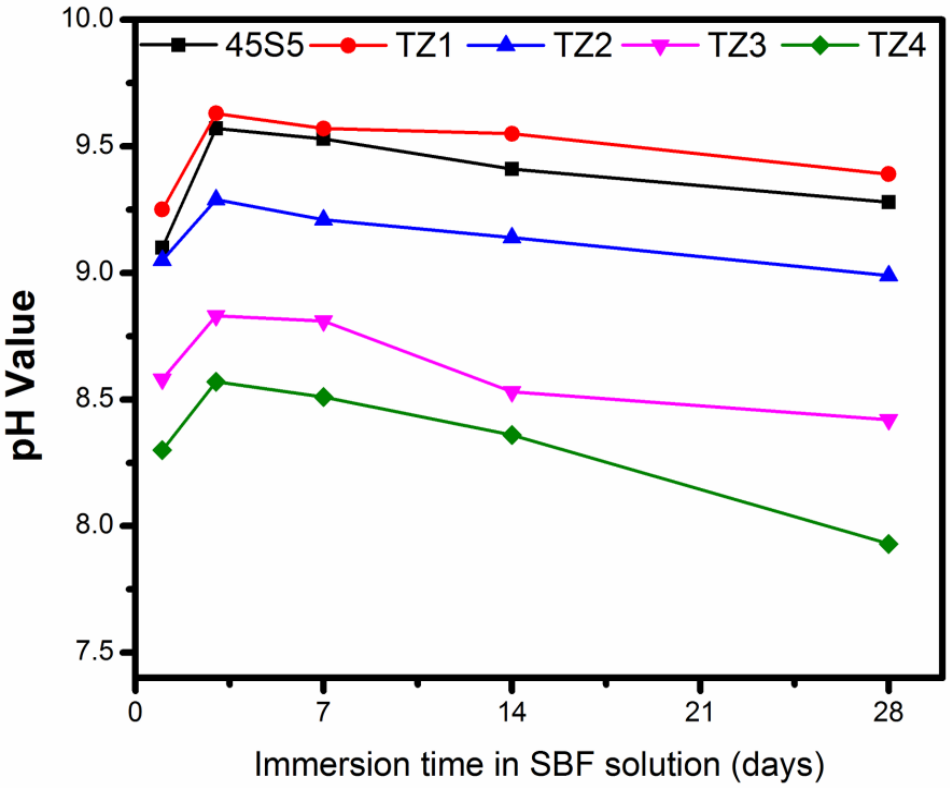

Fig. 7.3: Variation of pH of the SBF solution containing glass samples (45S5 to TZ4) with different time intervals.

The change in pH was due to ion leaching. The increase in pH of SBF solution shows a decrease in the concentration of H^+ ions due to the replacement of cations in the bioactive glass. It was also seen that the decrease in the pH of the SBF solution after 15 days as a result of breaking of glass network. Morphological properties of bioactive glasses also indicate that soaking in SBF lead to the formation of an apatite layer (Hayakawa *et al*., 1999 and Kasuga *et al*., 2001) on the surface of the samples. There are five proposed stages for HA formation in body fluid in simulated body fluid (SBF) *in vitro* (Hench, 1991 and Clark *et al*., 1976).

1. Rapid cation exchange of Na^+ and/or Ca^{2+} with H^+ from solution, creating silanol bonds (Si–OH) on the glass surface:

$Si\text{-}O^-Na^+ + H^+ + OH^- \longrightarrow Si\text{-}OH + Na^+(aq) + OH^-$

The pH of the solution increases and a silica-rich (cation-depleted) region forms near the glass surface. Phosphate is also lost from the glass if present in the composition.

2. High local pH leads to attack of the silica glass network by OH^-, breaking Si–O–Si bonds. Soluble silica is lost in the form of $Si(OH)_4$ to the solution, leaving more Si–OH (silanols) at the glass–solution interface:

$Si\text{-}O\text{-}Si + H_2O \longrightarrow Si\text{-}OH + OH\text{-}Si$

3. Condensation of Si–OH groups near the glass surface: repolymerization of the silica-rich layer.

4. Migration of Ca^{2+} and PO_4^{3-} groups to the surface through the silica-rich layer and from the solution, forming a film rich in amorphous $CaO–P_2O_5$ on the silica-rich layer.

5. Incorporation of hydroxyls and carbonate from solution and crystallization of the $CaO–P_2O_5$ film to HA.

7.3.4 SEM analysis of bioactive glass samples.

7.3.4.1 SEM analysis of bioactive glass samples before soaking in SBF solution

The SEM micrographs of bioactive glass samples before soaking in SBF solution are shown in Fig. 7.4 which shows different rod type structure and irregular grain of bioactive glass samples which is quite similar to the result found by Hanan *et al*. (Hanan *et al*., 2009).

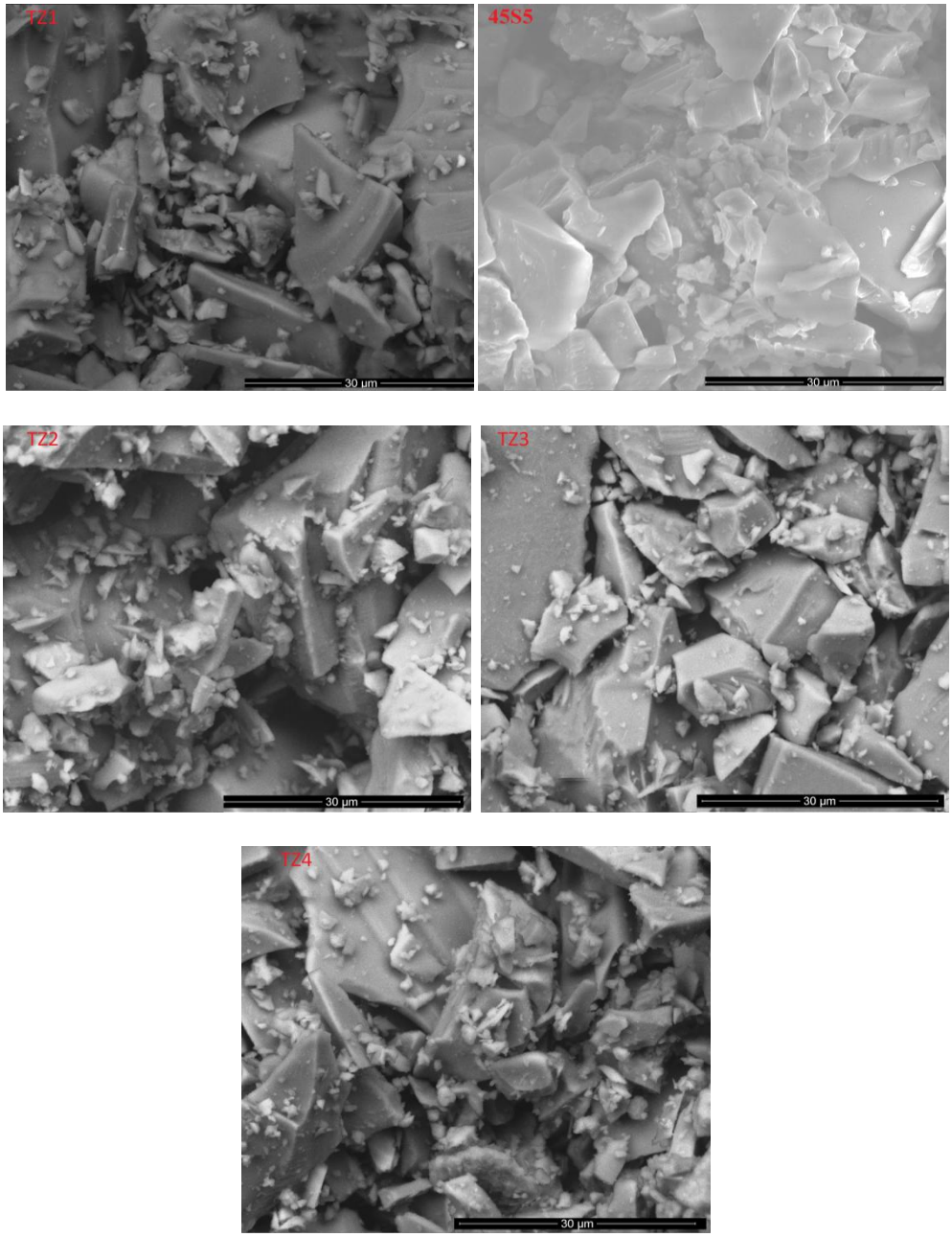

Fig. 7.4: SEM micrographs of bioactive glass samples (45S5 to TZ4) before soaking in SBF solution.

7.3.4.2 SEM analysis of bioactive glass samples after soaking in SBF solution

Fig. 7.5 shows the SEM micrographs of bioactive glass samples after soaking in SBF solution for 14 days. It is clear from the Fig. 7.5 that bioactive glass sample which were

soaked in SBF solution for 14 days were covered with irregular shape and grounded HA particles have been grown into several agglomerates consisting of needle-shaped HA layer. These micrographs show the formation of HA on the surface of bioactive glass samples after immersion in SBF solution for 14 days.

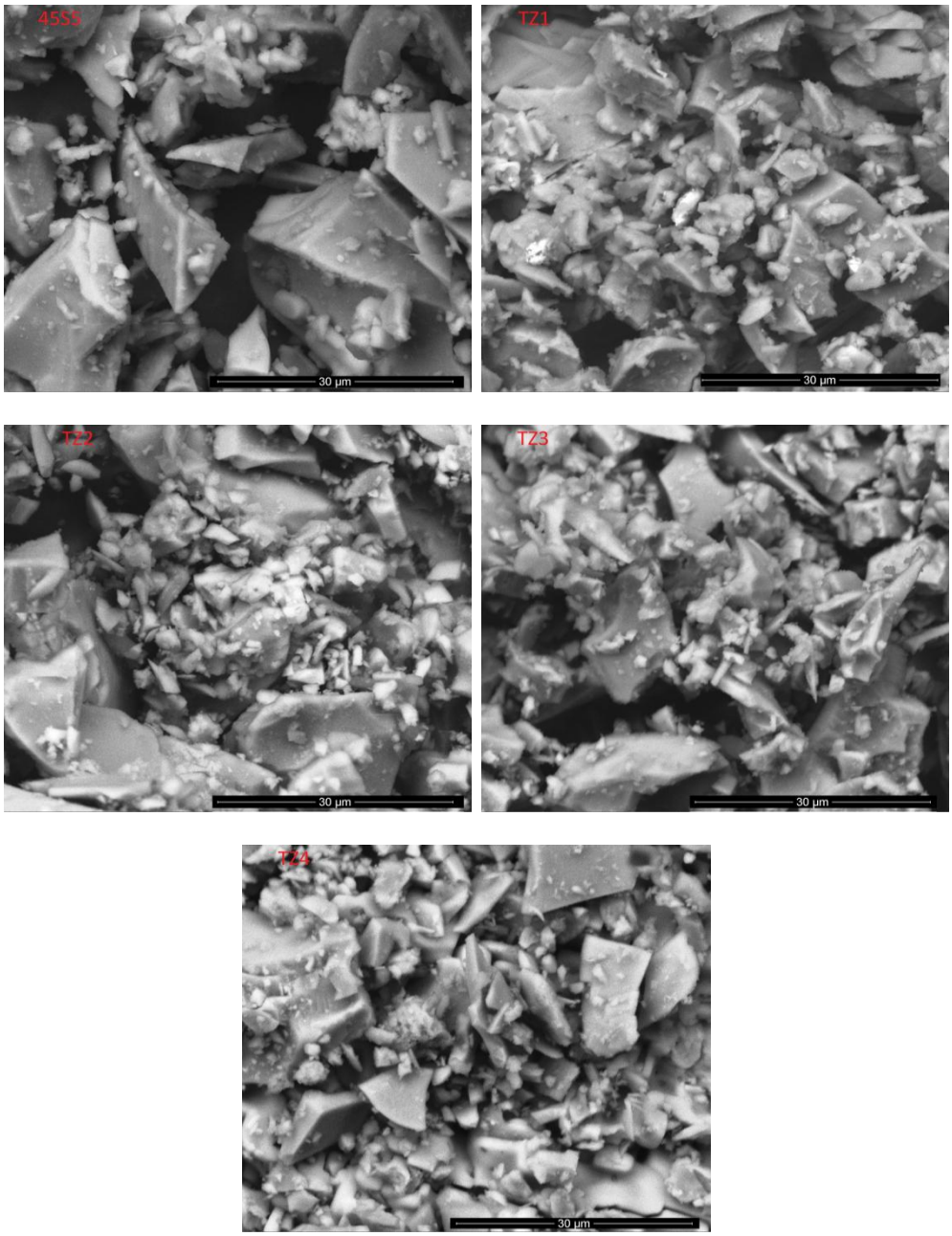

Fig. 7.5: SEM micrographs of bioactive glass samples (45S5 to TZ4) after soaking in SBF solution.

7.3.5 Transmission –FTIR analysis of bioactive glass samples before and after immersion in SBF solution

Fig. 7.6-7.10 show the corresponding transmission FTIR analysis of bioactive glass samples before and after immersion in SBF solution for 1 to14 days. The transmission spectra of all bioglass samples before soaking them in SBF solution exhibits vibrational bands at around 440 cm^{-1} due to Si-O-Si bending (Tripathi *et al*., 2015).

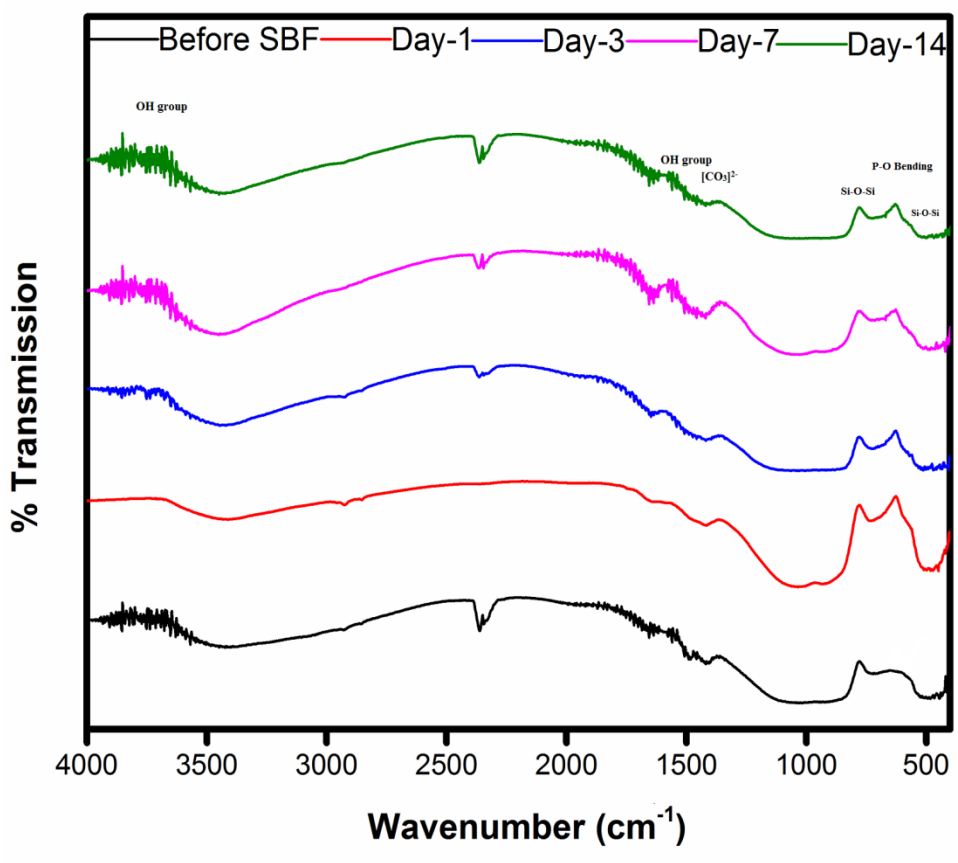

Fig. 7.6: FTIR transmission spectra of 45S5 bioactive glass sample before and after SBF treatment.

The FTIR spectra of bioactive glass samples after soaking in simulated body fluid (SBF) solution for different times reveal Si-O-Si tetrahedral (840 - 720 cm^{-1}) which indicates the formation of the silica - rich layer. The presence of P - O bending (amorphous) (560 -

550 cm^{-1}) bands indicates the formation of calcium phosphate (CaO - P_2O_5) layer (ElBatal *et al*., 2003). In addition to these other bands were also found to be centered at around 1420 and 1480 cm^{-1} which are attributed due to carbonate groups $(CO_3)^{2-}$ indicating the precipitation of B-type hydroxy carbonate apatite, $(Ca_9(HPO_4)_{0:5}(CO_3)_{0:5}(PO_4)_5OH)$ (HCA) mimicking bone like apatite in the system (Anthony *et al*., 2015).

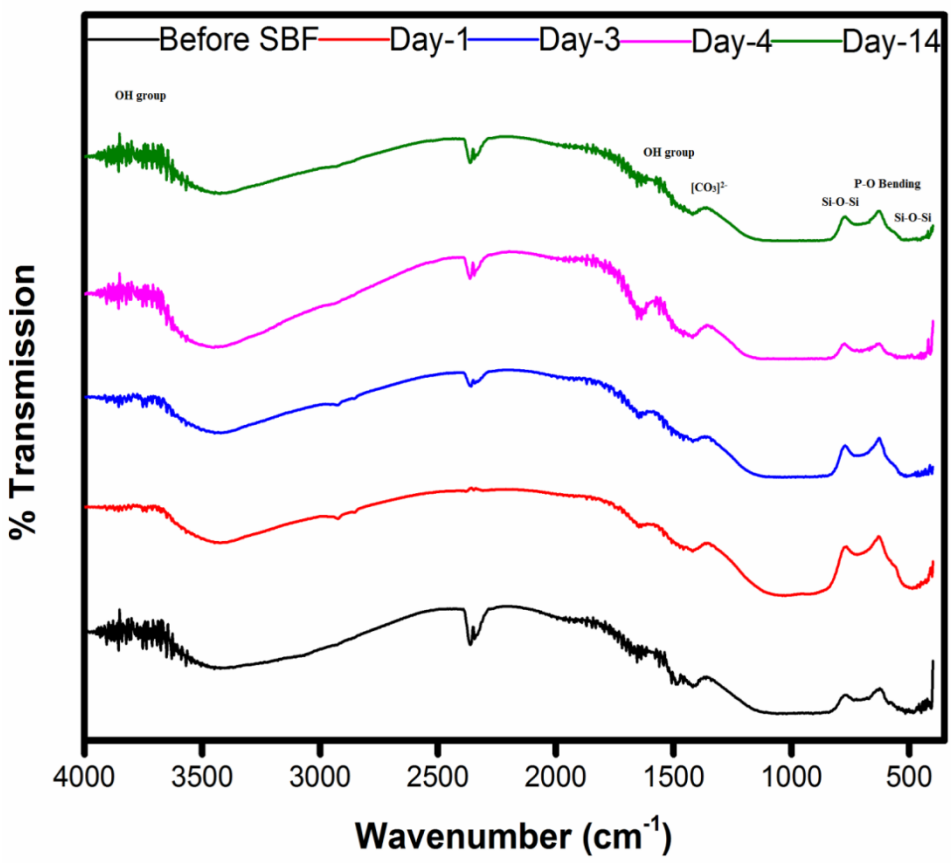

Fig. 7.7: FTIR transmission spectra of bioactive glass sample TZ1 before and after SBF treatment.

The presence of carbonate groups $(CO_3)^{2-}$ (1400-1500 cm^{-1}) bands show the crystalline nature of HA layer and their bands are attributed due to HA layer (Filgueiras *et al*., 1993

and Filho *et al*., 1996). The bands were observed at 1560 & above 3500 cm^{-1} in the spectra which are attributed due to presence of OH group because of water adsorption in the system (Stoch *et al*., 1999). Intensity of silica – rich layer and CaO - P_2O_5 layer goes on decreasing but the intensity of HA layer increases with time in all cases after soaking for 1 day in SBF solution.

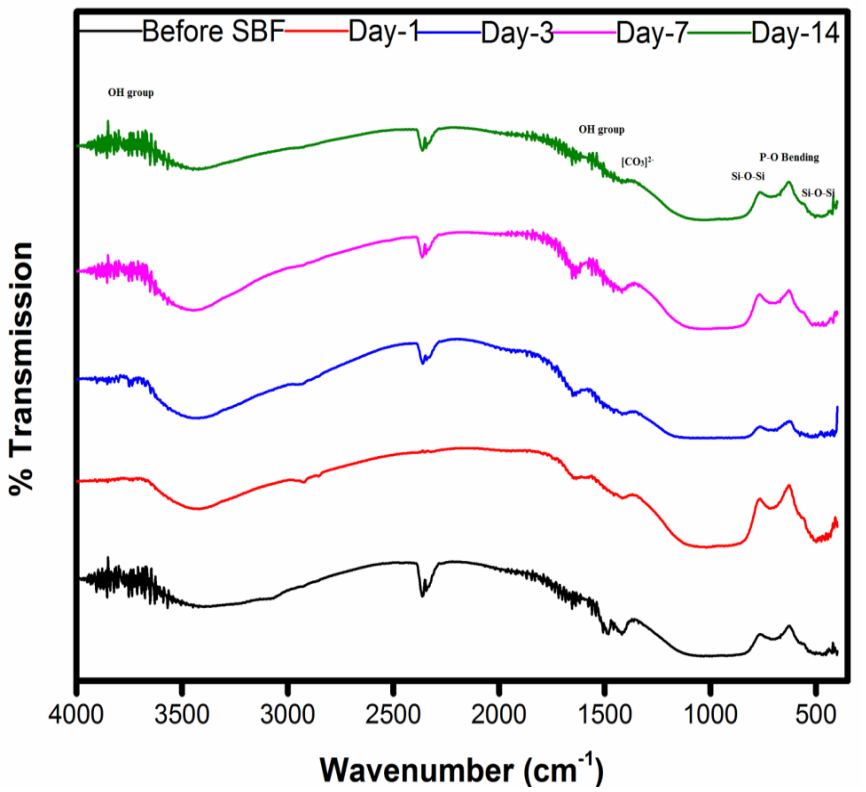

Fig. 7.8: FTIR transmission spectra of bioactive glass sample TZ2 before and after SBF treatment.

Hench et. al. (Hench et. al., 2006) was the first to detail a number of sequential steps in the *in vitro* and *in vivo* reactivity of silicate glasses that are responsible for the tissue bonding ability of these glasses. Briefly, these involve cation release from the glass with a consequential increase in pH of solution, formation of silica - rich layer and precipitation of a CaO - P_2O_5 rich layer that further crystallizes as HA layer (Hench, 1991

and Balamurugan *et al*., 2007).The degree of bioactivity is expressed by the formation of HA layer. Finally, the FTIR reflectance spectra of bioactive glasses after soaking for 14 days in SBF solution (Fig. 7.6-7.10) indicates that addition of more than 1 mol% of (TiO_2+ZrO_2) in the base bioactive glass (45S5) decreases its bioactivity. This is because of the fact that transition metals enhance the chemical durability of silicate glasses (ElBatal *et al*., 2010). The precipitation of pure hydroxyapatite in SBF is likely to happen less because it is saturated with respect to slightly carbonated apatite, in which the orthophosphates are substituted with carbonates in the crystal lattice (Elliot *et al*., 1994).

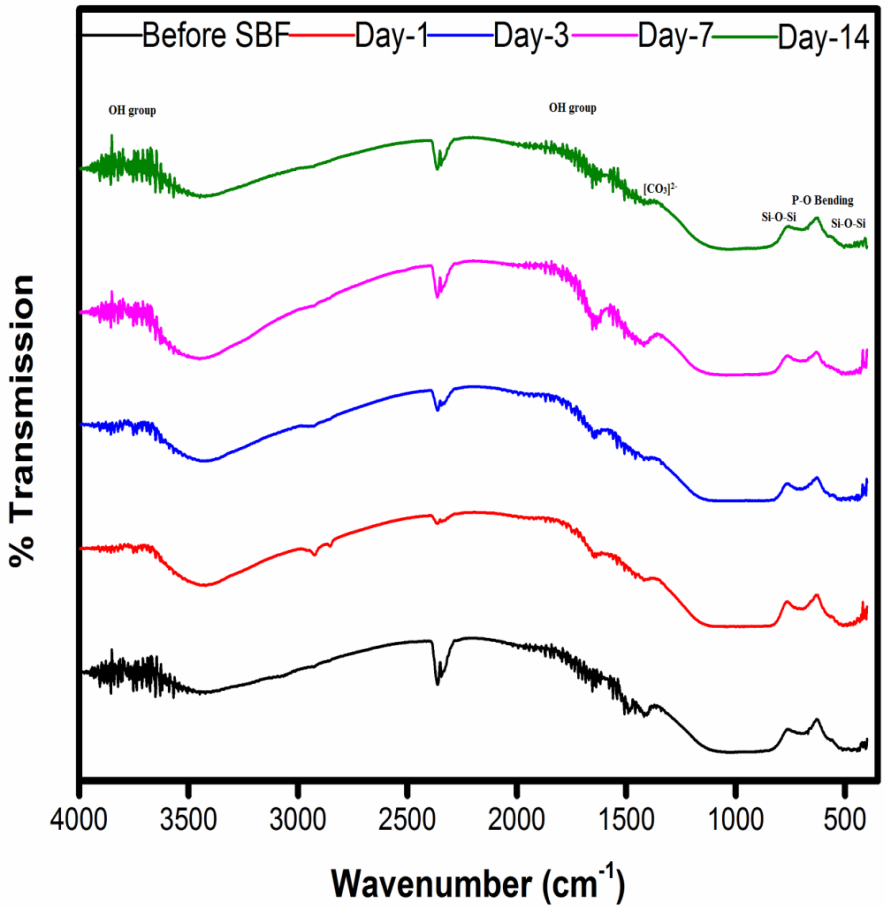

Fig. 7.9: FTIR transmission spectra of bioactive glass sample TZ3 before and after SBF treatment.

Gibson *et al* (Gibson *et al*., 2000) pointed out that the P-O bending bands, at 546 cm^{-1} in the FTIR spectra were not characteristic to HA or HCA, but they indicate the presence of orthophosphate lattices. Therefore, the phase formed at the surface of the bioactive glass samples were also confirmed by X-ray diffraction as shown in Fig 7.2. So our results regarding the formation of HCA in SBF by FTIR absorption spectrometry are well supported by the observations made by Anthony *et al* (Anthony *et al*., 2015).

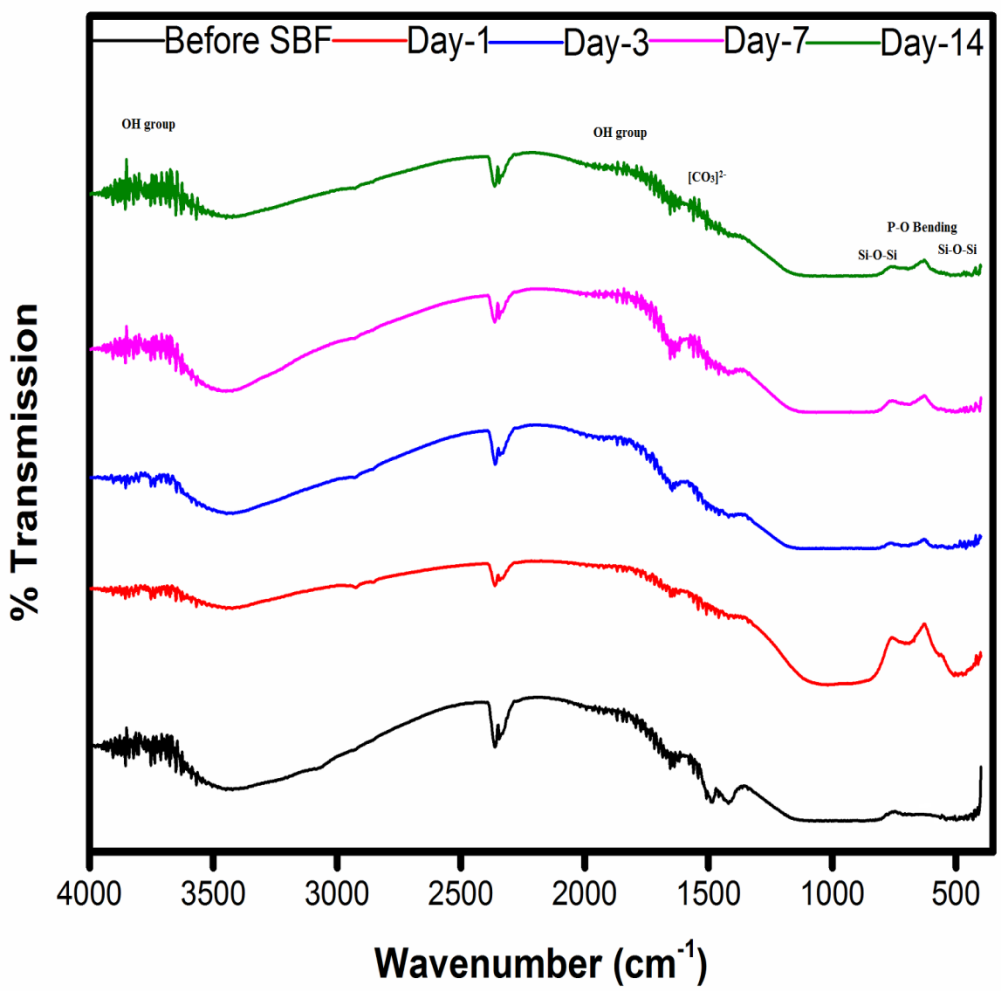

Fig. 7.10: FTIR transmission spectra of bioactive glass sample TZ4 before and after SBF treatment.

7.4. Conclusions

In the present investigation, a comparative study was made on physical, bioactive and mechanical properties of (TiO_2+ZrO_2) substituted 45S5 bioactive glasses. The following conclusions are obtained from this investigation:

1. On increasing the substitution of (TiO_2+ZrO_2) for SiO_2 in the bioactive glass 45S5, density and compressive strength were found to increase accordingly.

2. The transmission FTIR spectra showed different characteristics band because of silicate network which indicated the formation of the hydroxy calcium apatite (HA) layer on the surface of bioactive glass samples after immersing in SBF from 1 to 28 days.

3. The bioactivity of these samples was measured by in-vitro analysis in SBF solution for 1 to 28 days. The pH of the solution was found to increase from 1 to 3 days and nearly constant up to 7 days. After 7 days the pH of the glass samples decreased that shows the samples were bioactive. An increase in the pH of the SBF shows the relative increase in bioactivity of the sample immersed in the solution. Because the increase in pH values of the solution is due to fast release of cations through exchange with H^+ or H_3O^+ ions in the simulated body fluid (SBF) solution. The H^+ ions are being replaced by cations which cause an increase in hydroxyl ion (OH^-) concentration of the solution due to formation of their hydroxides. This leads to attack on the silica glass network, which results silanols (Si-OH) formation in the solution. Further condensation and repolymerization of silanols occurs at glass surface which results the formation of SiO_2 - rich layer. The migration of Ca^{2+} and PO_4^{3-}ions from the solution takes place on silica rich layer and form amorphous CaO-P_2O_5 layer. The incorporation of carbonate ions $(CO_3)^{2-}$ from the solution into amorphous CaO-P_2O_5 layer results in the formation of crystalline hydroxy carbonate

apatite layer (HCA) on the surface of the glass samples. Thus, the surface of the glass samples is covered by the bioactive HCA (Ca_{10} $(PO_4)_{6-x}$ $(CO_3)_x$ $(OH)_{2-x}$ where $0 \leq x \leq 2$) interface. The formation of HCA layer on the surface of the glass sample causes the termination of the contact between the sample and the SBF solution. This leads to a decrease in pH of the solution after 3 days as indicated in the Fig. 7.3 when bioactive glass samples were immersed in simulated body fluid (SBF) solution up to 28 days. The high degradation rate leads to higher pH value. Based on the above mechanism, an increase in the pH value of SBF solution also favors the hydroxy carbonate apatite formation leading to an increase in bioactivity of the samples.

5. The addition of (TiO_2+ZrO_2) beyond 1 mol% caused a decrease in maxima of the pH of the SBF solution containing immersed samples. This dictates that addition of (TiO_2+ZrO_2) up to 1 mol% in the glass samples has increased its bioactivity, but beyond 1 mol% of (TiO_2+ZrO_2) retards the bioactivity of the glass samples (Fig. 7.3).

4. The SEM analysis of these samples before soaking in SBF shows the different irregular grains of glass samples. While after 14 days of SBF treatment, HA layer was formed on the surface of these samples due to its bioactive nature.

Thus, we can say that substitution of (TiO_2+ZrO_2) for SiO_2 in the bioactive glass 45S5 would be good bioactive materials which have more mechanical properties with the comparison to bioactive glass 45S5.

References:

Abou Neel EA, Pickup DM, Valappil SP, Newport RJ and Knowles JC, Bioactive functional materials: a perspective on phosphate-based glasses, J Mater Chem, 19, 690–701, 2009.

Agathopoulos S, Tulaganov DU, Ventura JMG, Kannan S, Karakassides MA and Ferreira JMF, Formation of hydroxyapatite onto glasses of the CaO-MgO-SiO_2 system with B_2O_3, Na_2O, CaF_2 and P_2O_5 additives, Biomaterials, 27, 1832, 2006.

Anthony LB Macon, Taek B Kim, Esther M Valliant, Kathryn Goetschius, Richard K Brow, Delbert E Day, Alexander Hoppe, Aldo R Boccaccini, Ill Yong Kim, Chikara Ohtsuki, Tadashi Kokubo, Akiyoshi Osaka, Maria Vallet-Regı´, Daniel Arcos, Leandro Fraile, Antonio J Salinas, Alexandra V Teixeira, Yuliya Vueva, Rui M Almeida, Marta Miola, Chiara Vitale-Brovarone, Enrica Verne, Wolfram Holand and Julian R. Jones, A unified in vitro evaluation for apatite-forming ability of bioactive glasses and their variants, J Mater Sci: Mater Med, 26, 115, 2015.

Arstila H, Hupa L, Karlsson KH and Hupa M, Influence of heat treatment on crystallization of bioactive glasses, Journal of Non-Crystalline Solids, 354, 722–728, 2008.

Balamurugan A, Balossier G, Kannan S, Michel J, Rebelo AHS and Ferreira JMF, Development and in vitro characterization of sol - gel derived CaO - P_2O_5 - SiO_2- ZnO bioglass, Acta Biomaterialia, 3, 255 – 262, 2007.

Bharati S, Soundrapandian C, Basu D and Datta S, Studies on a novel bioactive glass and composite coating with hydroxyapatite on titanium based alloys: Effect of γ-sterilization on coating, J European Ceram Soc, 29, 2527–2535, 2009.

Cao W and Hench LL, Bioactive Materials, Ceramics International, 22, 493–507, 1996.

Clark and Hench LL, The influence of surface chemistry on implant interface, J Biomed Mater Res, 10, 161-74,1976.

Clark AE, Pantano CG and Hench LL, Auger spectroscopic analysis of Bioglass corrosion films, J Am Ceram Soc, 59, 37–39, 1976.

ElBatal HA, Azooz MA, Khalil EMA, Soltan Monem A and Hamdy YM, Characterization of some bioglass–ceramics, Materials Chemistry and Physics, 80, 599–609, 2003.

ElBatal FH, Khalil EM, Hamdy YM, Zidan HM, Aziz MS and Abdelghany AM, FTIR Spectral Analysis of Corrosion Mechanisms in Soda Lime Silica Glasses Doped with Transition Metal Oxides, Silicon, 2, 41 – 47, 2010.

Elliot JC, editor. Structure and chemistry of the apatites and other calcium orthophosphates, Amsterdam: Elsevier Science, 1994.

Filgueiras MR, LaTorre GP and Hench LL, Solution effects on the surface reactions of three bioactive glass compositions, Journal of Biomedical Materials Research, 27, 1485 - 1493, 1993.

Filho OP, LaTorre GP and Hench LL, Effect of crystallization on apatite layer formation of bioactive glass 45S5, Journal of Biomedical Materials Research, 30, 509 - 514, 1996.

Gisbon IR, Rehman I, Best SM and Bonfield W, Characterization of the transformation from calcium-deficient apatite to b-tricalcium phosphate, J Mater Sci, 12, 799–804, 2000.

Greenspan DC and Hench LL, Chemical and mechanical behavior of bioglass coated alumina, J Biomed Materials Res, 10, 503–509, 1976.

Habibe AF, Maeda LD, Souza RC, Barboza MJR, Daguano JKMF, Rogero SO and Santos C, Effect of bioglass additions on the sintering of Y-TZP bioceramics, Mater Sci Eng C, 29, 1959–1964, 2009.

Hanan H Beherei, Khaled R Mohamed and Gehan T El-Bassyouni, Fabrication and characterization of bioactive glass (45S5)/titania biocomposites, Ceramics International, 35, 1991-1997, 2009.

Hench LL, Bioceramics: From concept to clinic, J Am Ceram Soc, 74, 1487-1510, 1991.

Hench LL, The story of Bioglass, J Mater Sci Mater Med, 17, 967-978, 2006.

Hench LL, Splinter RJ, Allen WC and Greenlee TK, Bonding mechanisms at the interface of ceramic prosthetic materials, J Biomed Mater Res Symp, 334, 117–41, 1971.

Jung SB, Day DE, Day T, Stoecker W and Taylor P, Treatment of non-healing diabetic venous stasis ulcers with bioactive glass nanofibers, Wound Repair Regen,19, 30, 2011.

Kokubo K, Ito S, Huang ZT, Hayashi T, Sakka S, Kitsugi T and Yamamuro T, Solutions able to reproduce in vivo surface-structure changes in bioactive glass– ceramics A–W, Journal of Biomedical Materials Research, 24, 721– 734, 1990.

Kokubo T, Bioactive glass-ceramics – properties and applications, Biomaterials, 12, 155–63, 1991.

LeGeros RZ, Properties of osteoconductive biomaterials: calcium phosphates, Clin Orthop Relat Res, 395, 81–98, 2002.

Li P, Zhang F, Kokubo T, The effect of residual glassy phase in a bioactive glass–ceramic on the formation of its surface apatite layer in vitro, Journal of Materials Science: Materials in Medicine, 3, 452–456, 1992.

Marti, Dr. Robert Mathys Foundation, Bischmattstr. 12, CH-2544 Bettlach, Inert bioceramics (Al_2O_3, ZrO_2) for medical application, Injury-international Journal of The Care of The Injured - INJURY-INT J CARE INJURED 01/2000; 31. DOI:10.1016/S0020-1383(00)80021-2

Rahaman MN, Day DE, Bal BS, Fu Q, Jung SB and Bonewald LF, Bioactive glass in tissue engineering. Acta Biomater , 7, 2355–73, 2011.

Satoshi Hayakawa, Kanji Tsuru, Chikara Ohtsuki and Akiyoshi Osaka, Mechanism of Apatite Formation on a Sodium Silicate Glass in a Simulated Body Fluid, J Am Ceram Soc, 82, 2155–2160, 1999.

Singh D, de la Cinta Lorenzo-Martin M, Gutiérrez-Mora F, Routbort JL and Case ED, Self-joining of zirconia/hydroxyapatite composites using plastic deformation process, Acta Biomater, 2, 669-675, 2006.

Stoch A, Jastrzebski W, Brozek A, Trybalska B, Cichocinska M and Szarawara E, FTIR monitoring of the growth of the carbonate containing apatite layers from simulated and natural body fluids, Journal of Molecular Structure, 511–512, 287–294, 1999.

Toshihiro Kasuga, Yoshimasa Hosoi, Masayuki Nogami and Mitsuo Niinomi, Apatite Formation on Calcium Phosphate Invert Glasses in Simulated Body Fluid, J Am Ceram Soc, 84, 45-52, 2001.

Tripathi Himanshu, Kumar Sampath A and Singh S P, Preparation and characterization of $Li_2O–CaO–Al_2O_3–P_2O_5–SiO_2$ glasses as bioactive material, Bull Mater Sci, 39(2), 365–376, 2016.

Tripathi Himanshu, Hira Sumit Kumar, Kumar Sampath A, Gupta Uttam, Manna Partha Pratim and Singh S P, Structural characterization and *in vitro* bioactivity assessment of SiO_2–CaO–P_2O_5–K_2O–Al_2O_3 glass as bioactive ceramic material, Ceramics International, 41, 11756–11769, 2015.

Shirtliff VJ and Hench LL, Bioactive materials for tissue engineering, regeneration and repair, Journal of Materials Science, 38, 4697–4707, 2003.